ELSEVIER

Materials Chemistry and Physics 77 (2002) 647–654

MATERIALS CHEMISTRY AND PHYSICS

www.elsevier.com/locate/matchemphys

Preparation and cathodoluminescence of ZnO phosphor

C.H. Lin [a], Bi-Shiou Chiou [a,*], C.H. Chang [a], J.D. Lin [b]

[a] *Department of Electronics Engineering and Institute of Electronics, National Chiao Tung University, Hsinchu 300, Taiwan*
[b] *Electronic Research Service Organization, Industrial Technology Research Institute, Hsinchu, Taiwan*

Received 27 July 2001; received in revised form 2 January 2002; accepted 15 January 2002

Abstract

Zinc oxide phosphors (ZnO:Zn) were prepared with solid state sintering of ZnO powders with ZnS and screen printed onto ITO-coated glass substrates to form a thin layer. Structural characterization carried out by X-ray diffraction (XRD) analysis suggests that the Zn atoms originated from the decomposition of ZnS, and diffuse to occupy the oxygen vacancies in the host lattice. Both lattice parameters *a* and *c* decrease slightly with the increase of ZnS content and/or firing temperature. The cathodoluminescent (CL) peak band varies with ZnS content and ranges from 494 to 508 nm, which is close to the green band of ZnO phosphor. Various mechanisms have been proposed in literatures to explain the origin of the green emission band. Among them, the presence of oxygen vacancies and trace ZnS residue are possible causes for the green emission in this study. CL spectra and CIE color loci suggest that ZnO:Zn phosphor with 5 wt.% ZnS can be used as a green primary for color picture tubes.

Keywords: Zinc oxide phosphors; Cathodoluminescent; CIE

1. Introduction

Phosphors are materials that emit photons with a high efficiency. They are widely used as radiation detectors and in visual displays such as computer monitors and television screen. Given the recent thrust of activity in the flat panel display area, it is imperative to optimize phosphor properties to reduce power consumption and increase brightness [1–4].

As a wide band-gap material, ZnO has an electronic structure which makes it a useful candidate for luminescent devices. Recently, ZnO has regained considerable interest because of its potential use in new low voltage luminescence applications such as field emission displays (FEDs) [5]. Pure ZnO emits a narrow luminescence band in the blue–violet spectral region [6]. However, upon incorporation of various dopants, a variety of emissions, ranging from blue to orange spectral region occur [7].

In this research, ZnO doped with Zn (ZnO:Zn) phosphors were prepared by solid state sintering of ZnO powders with various amounts of zinc sulfide (ZnS) at various temperatures in nitrogen atmosphere. The effects of sintering temperature and ZnS content on the phosphor powder shape, powder size distribution, lattice parameters, and luminescent characteristics of phosphors were investigated. Mechanisms for the green emission of ZnO:Zn phosphor are discussed.

* Corresponding author.
E-mail address: bschiou@cc.nctu.edu.tw (B.-S. Chiou).

2. Experimental

Zinc-doped zinc oxide was prepared by solid state sintering of mixtures of ZnO and ZnS powders in N_2 atmosphere at temperatures ranging from 800 to 1200 °C for 1 h. N_2 atmosphere was employed because previous study on the effect of sintering ambient suggested that specimens sintered in N_2 had higher brightness and better CIE color. The as-sintered powders were examined with a scanning electron microscope (SEM, Leica S440, Japan) to investigate the particle size, shape and surface morphology. The phosphor powder was further examined with a laser particle size analyzer (Analysette 22, Fritsch) to evaluate the particle size distribution. The phase and crystal structure of the as-fabricated phosphor were identified with an X-ray diffractometer (Rigaku Ru-200, Japan) with a wavelength of Cu Kα ($\lambda = 1.5406$ Å). The scanning rate was $4^\circ\,\mathrm{min}^{-1}$.

Screen printing method was employed to deposit the phosphor powders onto indium–tin-oxide (ITO) coated glass. Paste consisting of polyvinyl alcohol (PVA, as a binder) and as-sintered phosphor was printed onto ITO glass and baked at 450 °C for 1 h. The film thickness was about 100 μm.

The cathodoluminescence (CL) spectra were measured with an electron gun in a vacuum chamber. The chamber was pumped down to 5×10^{-2} Torr with a mechanical pump and to 5×10^{-7} Torr with a turbo pump. Samples were excited by electron beam with an accelerating voltage of 1 kV

0254-0584/02/$ – see front matter
PII: S0254-0584(02)00120-7

and electron current of 10 μA. The beam size was 1.5 mm diameter. The CL emission light passes through a lens to focus on an optical fiber and is converted to an electrical signal by Fourier transform analysis instruments. The CL intensity was measured with a CL–SEM system (Nicolet MX-1, Acton Research Corporation) with a voltage from 0 to 20 kV. The wavelength detection range was 300–700 nm. The CIE color coordinates were measured with a colorimeter (Minolta CS-100, Japan) and the electron gun employed in the CL measurement.

3. Results and discussion

The X-ray diffraction (XRD) patterns of ZnO with various amounts of ZnS sintered in nitrogen atmosphere at 1100 °C for 1 h are given in Fig. 1. Along with the usual reflection of the hexagonal phase of ZnO, peaks of unreacted ZnS are also found for compositions with a ZnS content of 7 wt.% or larger. Fig. 2 shows XRD spectra of samples with 5 wt.% ZnS sintered in N_2 at various temperatures for 1 h. Samples fired at either 800 or 900 °C exhibit peaks corresponding to the ZnS phase, which indicates that the firing temperature should be above 1000 °C for 5 wt.% ZnS to react completely.

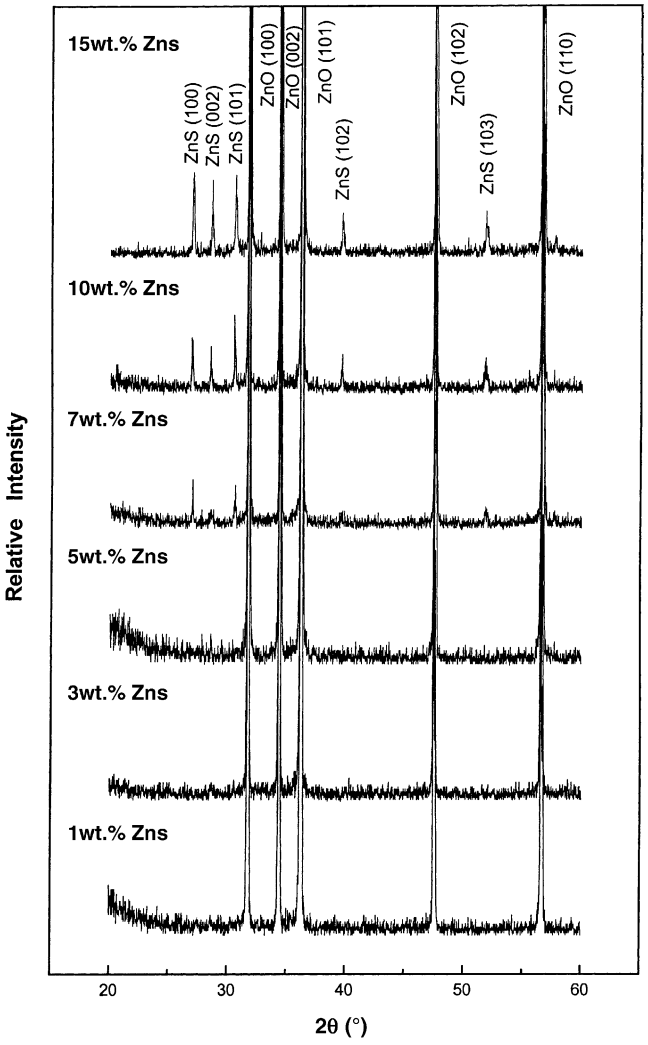

Fig. 1. The XRD patterns for ZnO with various amounts of ZnS sintered in N_2 at 1100 °C for 1 h.

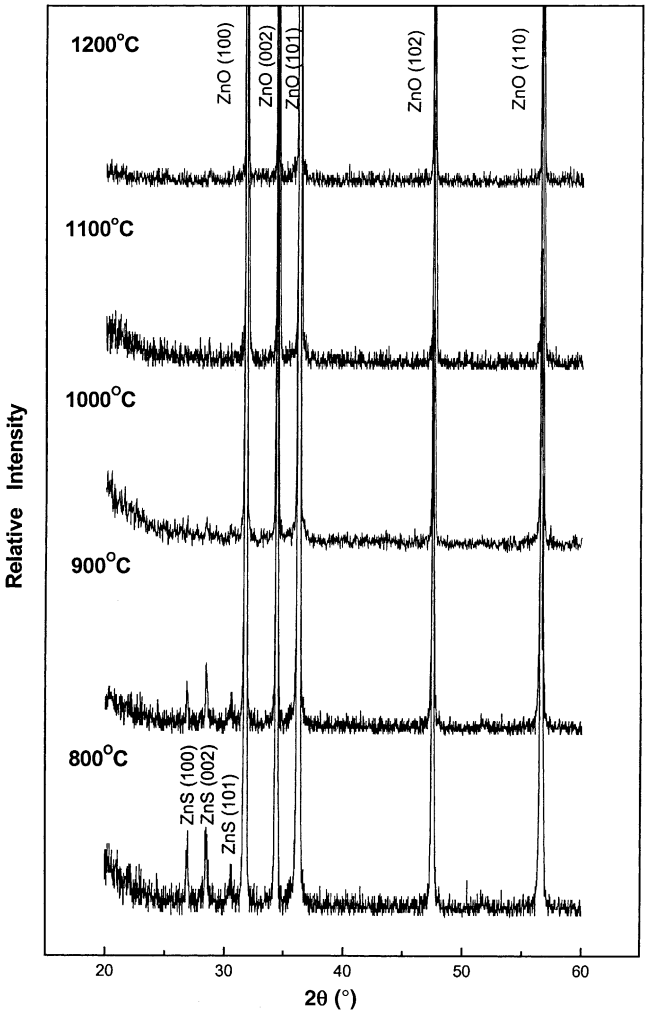

Fig. 2. The XRD patterns for ZnO with 5 wt.% ZnS sintered in N_2 at various temperatures for 1 h.

The average particle size of as-sintered (ZnO + ZnS) phosphor increases with the increase of firing temperature as shown in Fig. 3, while no apparent difference in particle size is observed for ZnO:Zn powders with various amounts of ZnS (Fig. 4).

On the basis of the XRD patterns shown in Figs. 1 and 2, the ZnS peaks disappear for samples sintered at a temperature ≧900 °C and with a ZnS content of ≦5 wt.%. The Zn atoms from the decomposition of ZnS may diffuse either to the interstitial sites or to the host lattices. For the former the reaction is as follows [7]:

$$\mathrm{ZnO} + x\mathrm{ZnS} \rightarrow \mathrm{Zn}(\mathrm{O}_{1-X} \cdot x V_{\mathrm{o}}) + x\mathrm{SO} + x\mathrm{Zn}_i^{2+} + 2x\mathrm{e}' \quad (1)$$

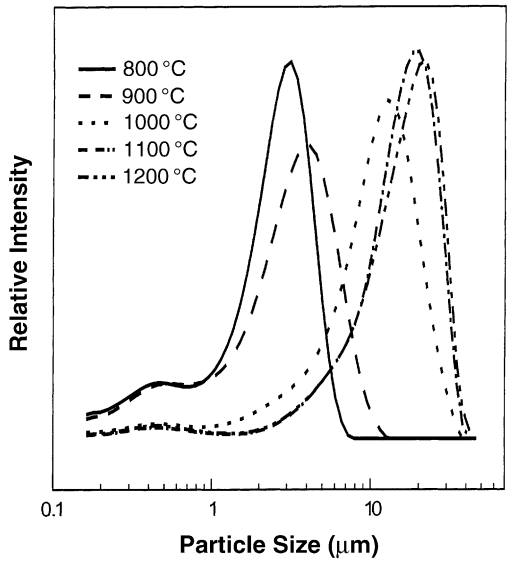

Fig. 3. Particle size distribution for ZnO:Zn sintered in N_2 at various temperatures for 1 h. Starting composition: 95 wt.% ZnO–5 wt.% ZnS.

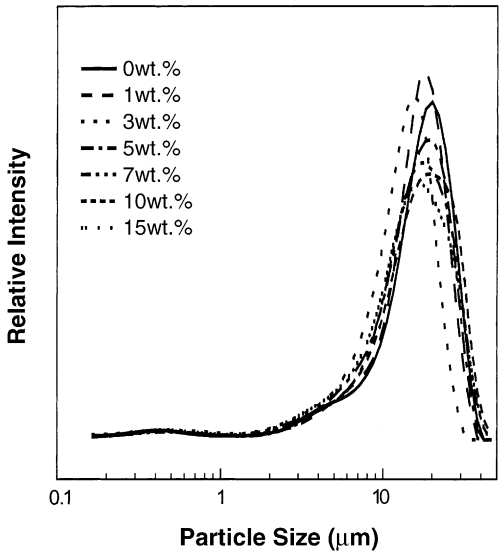

Fig. 4. Particle size distribution for ZnO with various amounts of ZnS sintered in N_2 at 1100 °C for 1 h.

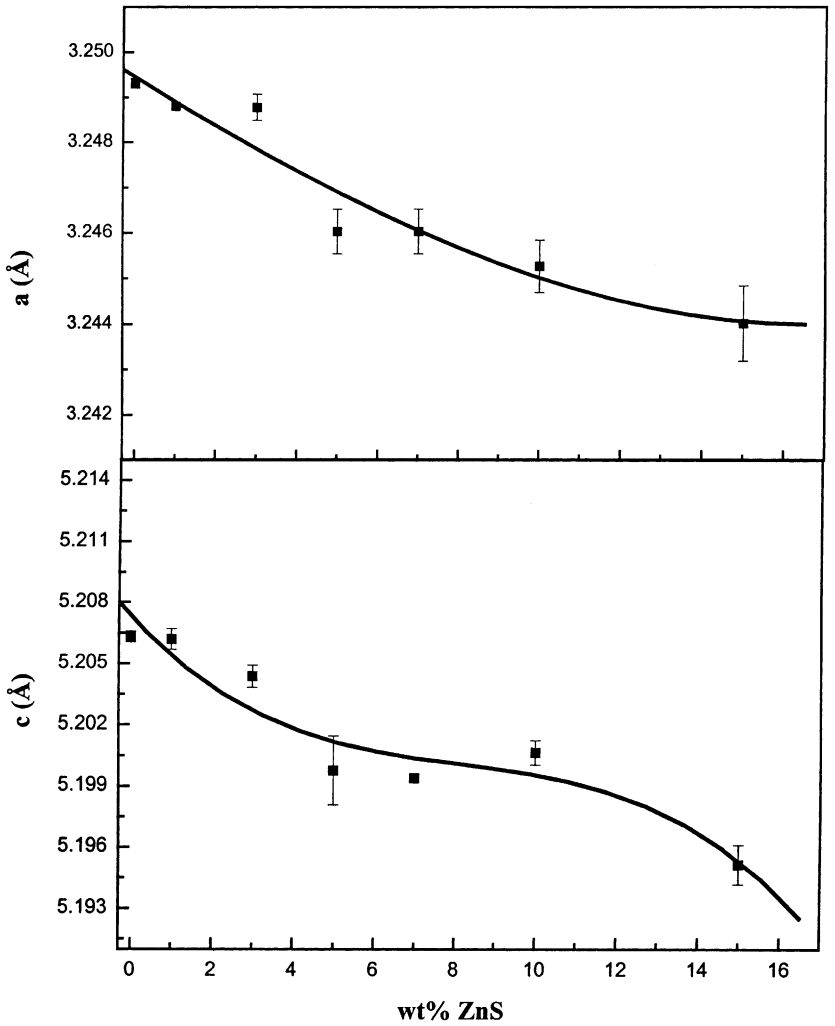

Fig. 5. Lattice parameters *a* and *c* of ZnO:Zn phosphors prepared with ZnO and various amounts of ZnS sintered in N_2 at 1100 °C for 1 h.

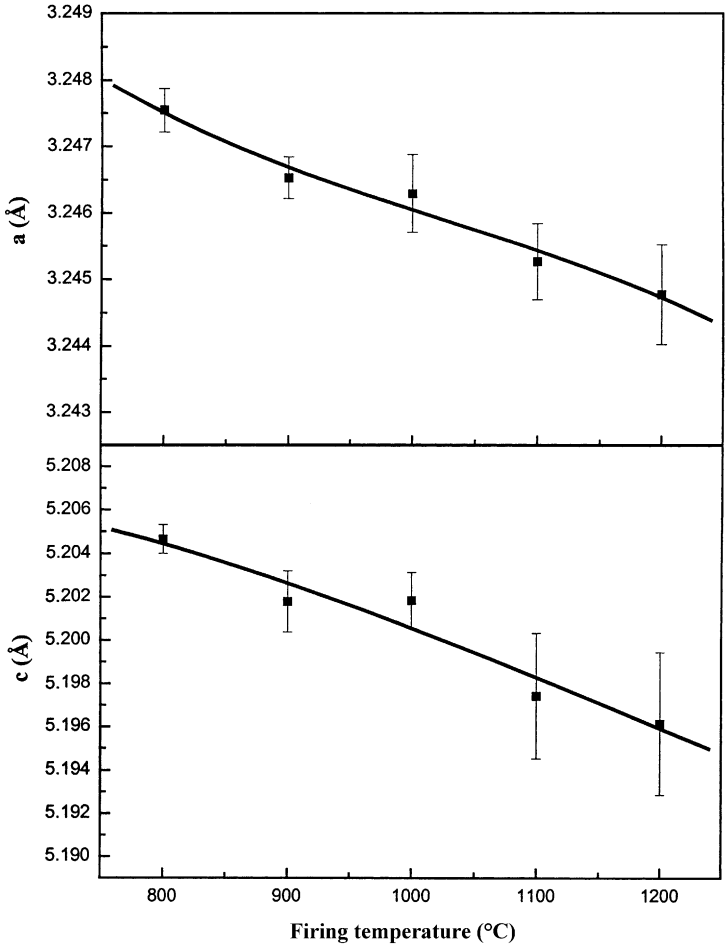

Fig. 6. Lattice parameters *a* and *c* of ZnO:Zn phosphors as a function of firing temperatures.

There are oxygen vacancies created in ZnO lattices and excess Zn atoms in the interstitial sites. However, as the radius of Zn is 0.75 Å and that of the oxygen vacancy is 1.4 Å [8], it is argued that Zn atom is too large to remain as an interstitial and possibly occupies the oxygen vacancy already created as shown in the following [9]:

$$\mathrm{ZnO} + x\mathrm{ZnS} \rightarrow \mathrm{Zn}(\mathrm{O}_{1-X} \cdot x\mathrm{V_o}) + x\mathrm{SO} + x\mathrm{Zn}_i{}^{2+} + 2x\mathrm{e}' \quad (1)$$

$$x\mathrm{Zn}_i{}^{2+} + 2x\mathrm{e}' \rightarrow x\mathrm{Zn}^0 \quad (2)$$

$$x\mathrm{Zn}^0 + x\mathrm{V_o} \rightarrow x\mathrm{Zn_o}{}^0 \quad (3)$$

$$\mathrm{ZnO}_{1-X} + x\mathrm{Zn_o}{}^0 \rightarrow \mathrm{ZnO}_{1-X} : x\mathrm{Zn_o}{}^0 \quad (4)$$

The defect formation behavior is one where the sulfide decomposes, reduces the host lattice and forms an oxygen vacancy plus two free electrons. These electrons then reduce the interstitial Zn^{2+} cations to the metal valance state Zn^0.

Figs. 5 and 6 are the lattice parameters of ZnO:Zn phosphor calculated on the basis of XRD data shown in Figs. 1 and 2, respectively. Both lattice parameters *a* and *c* decrease slightly (<0.2%) with the increase of ZnS content

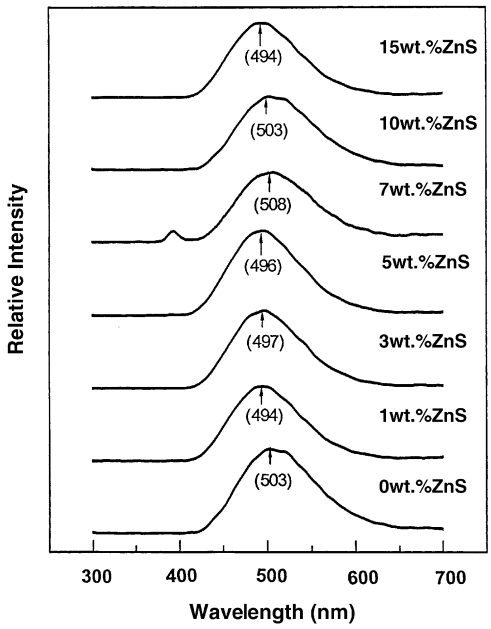

Fig. 7. CL spectra of ZnO:Zn phosphors prepared with ZnO and various amounts of ZnS sintered in N_2 at 1100 °C for 1 h. Samples measured at 1 kV and 10 μA. Number in parenthesis is the peak wavelength in nm.

and/or firing temperature. As stated previously, both zinc ion and oxygen vacancies are generated during firing of (ZnO + ZnS). The presence of Zn atoms in the interstitial tends to enhance the lattice parameters. As the lattice parameters decrease when more ZnS is consumed, it suggests that zinc atoms diffuses to occupy the oxygen vacancies, since the presence of Zn in the interstitial site would enhance the lattice parameters. Besides, the radius of Zn atom is smaller than that of oxygen vacancies, the more ZnS consumed (i.e., higher firing temperature or higher ZnS content), the smaller the lattice parameter, as observed. However, the above discussion must be regarded as speculative and not explicitly proven, even though it is consistent with the XRD results. Further investigation is needed to verify this defect formation mechanism.

Fig. 7 exhibits CL spectra of ZnO:Zn with various amounts of ZnS. The wavelength of emission ranges from 420 to 620 nm (corresponding to an energy 2.95–2 eV), and a shift in the peak luminescent band is observed among samples with various ZnS content as indicated in Fig. 7. Lehman reported that ZnO phosphor has four different luminescence bands, two intrinsic bands, 3.19 eV (388 nm, UV band) and 2.43 eV (510 nm, green band), and two extrinsic bands, 1.97 eV (629 nm, red band) and 1.35 eV

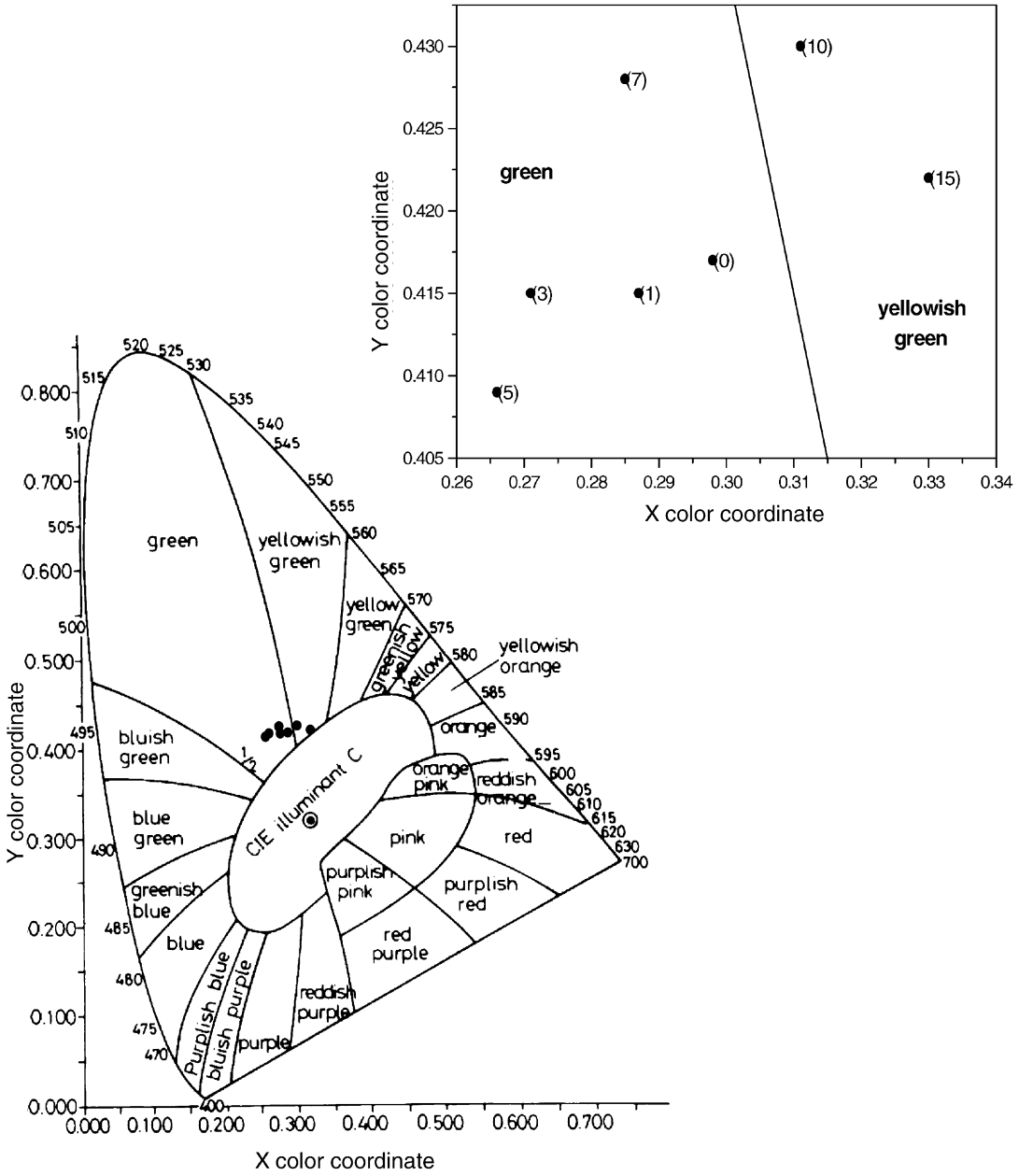

Fig. 8. CIE color loci of ZnO:Zn phosphors prepared with ZnO and various amounts of ZnS sintered in N_2 at 1100 °C for 1 h. Inset is the exploded view of the *X*- and *Y*-coordinates of specimens studied. The number in parenthesis is wt.% ZnS. CIE measured at 1 μA, 800 V.

(918 nm, infrared band). The extrinsic bands are caused by the chemical impurities. However, there are no reasonable models to explain the intrinsic luminescence bands. The observed peak band ranges from 494 to 508 nm, which is close to the green band of ZnO phosphor. Different mechanisms have been proposed to explain the origin of the green emission band, including the transition from Zn^{+} to Zn^{2+} in the excess of Zn ions, the involvement of O vacancies, interstitial O, Zn vacancies, Zn interstitials, a small amount of ZnS (≦0.1%) present in solid solution in ZnO, and even Cu impurities [10–13]. Recent works by Vanheusden et al. [11–13] report a strong correlation between the green 510 nm emission, the free-carriers concentration, and the density of singly ionized vacancies in commercial ZnO phosphor powders. They suggest that the green emission in ZnO phosphors is due to the recombination of an electron in singly occupied oxygen vacancies with photoexcited holes in the valence band. The XRD data and the calculated lattice parameters in this study suggest the diffusion of Zn interstitial into oxygen vacancies of the sintered phosphor as discussed previously. Hence, it is unlikely that the interstitial zinc be the center responsible for green luminescence. There are several possibilities for green emission in this study, such as presence of oxygen vacancies and trace ZnS residue as exhibited in the XRD patterns shown in Figs. 1 and 2. However, further investigation is needed to explore the green emission mechanism for ZnO:Zn phosphor.

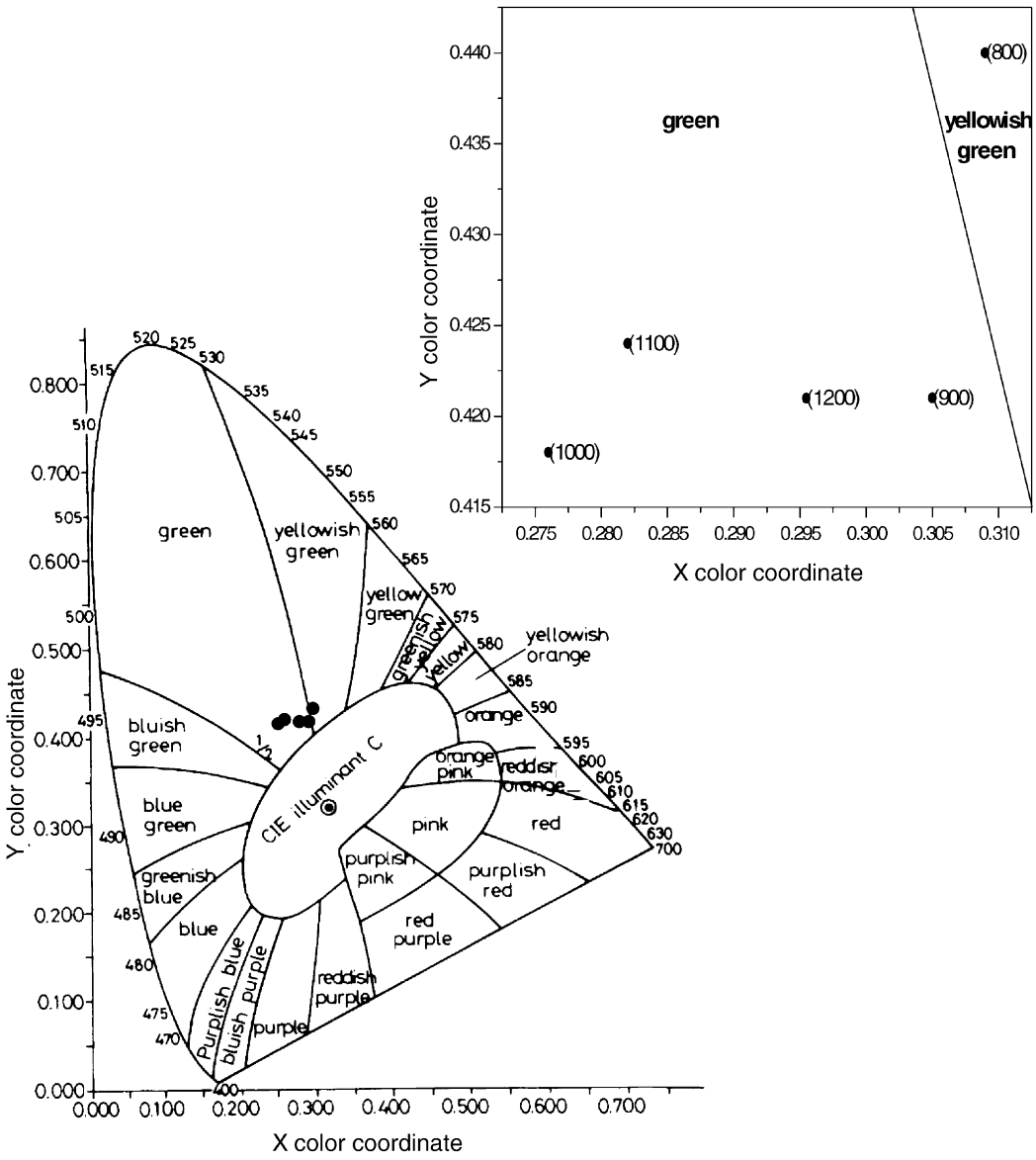

Fig. 9. CIE color loci of ZnO:Zn phosphor sintered in N_2 at various temperatures for 1 h. Inset is the exploded view of the *X*- and *Y*-coordinates of specimens studied. The number in parenthesis is the sintering temperature in °C. Starting composition: 95 wt.% ZnO–5 wt.% ZnS, CIE measured at 1 μA, 800 V.

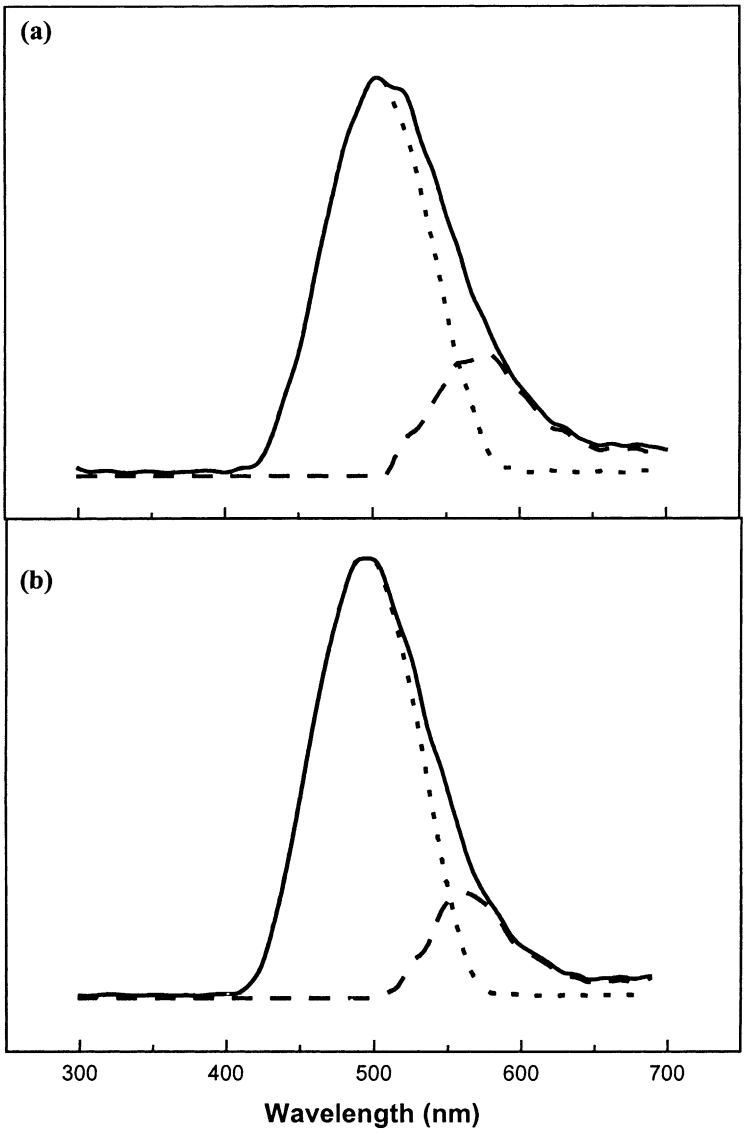

Fig. 10. CL spectra of ZnO:Zn phosphors with CL peak deconvoluted. Samples with (a) 0 wt.% ZnS and (b) 15 wt.% ZnS. (—) CL spectrum, (- - -) deconvoluted green emission (500 nm), (– – –) deconvoluted yellow emission (573 nm).

Table 1
CL peaks for ZnO:Zn phosphors prepared with ZnO:Zn and various amounts of ZnS

ZnS content (wt.%)	Position (nm)		Relative strengths (%)		Peak ratio (G/Y)
	G (green)	Y (yellow)	G	Y	
0	503	576	75.7	24.3	3.12
1	494	562	81.9	18.1	4.52
3	497	572	85.3	14.7	5.80
5	496	577	86.8	13.2	6.58
7	508	587	84.8	15.2	5.58
10	503	576	75.8	24.2	3.13
15	494	562	81.9	18.1	4.52

The CIE color coordinate is employed to analyze the luminescence color. As observed from the CIE color loci shown in Figs. 8 and 9, the color of ZnO:Zn phosphor changes with ZnS content and/or sintering temperature. Samples with less than 10 wt.% ZnS and sintered at 1100 °C are of green color. Among them the 5 wt.% specimen, located in the middle of the green region in the CIE loci, should provide a color that is more "green" than others (Fig. 8). Samples with ≧10 wt.% ZnS or sintered at 800 °C are of yellowish green color as shown in Figs. 8 and 9. The shift in color coordinates shown in Fig. 8 can be grouped into a cluster for ZnS ≦ 5 and >5 wt.% while that shown in Fig. 9 can be grouped for $T \geqq 900$ °C and $T < 900$ °C. The XRD data indicate that unreacted ZnS existed for specimens with ZnS > 5 wt.% and or sintered at $T < 900$ °C. The unreacted ZnS could serve as chemical impurity which causes the extrinsic yellow band [10] and results in the yellowish green color of the phosphor.

There is a shoulder on the longer wavelength side of the main peak for the CL spectra in all samples (Fig. 7). The deconvoluted CL spectra allow one to distinguish between a peak located at around 500 nm (referred to as G, green) and a peak around 573 nm (referred to as Y, yellow). The corresponding deconvoluted peaks are indicated by full curves as shown in Fig. 10. The resolution procedure for the CL peak uses two Gaussian functions with variable positions, width and intensities. Table 1 summarizes the corresponding results. The relative strengths are obtained by comparing the integrated area of the G and Y peaks. As can be seen in Table 1, the peak ratio G/Y of the 5 wt.% ZnS specimen is the largest among all compositions studied. This also suggests that ZnO:Zn phosphor with 5 wt.% ZnS can be used as a green primary for color picture tubes.

4. Conclusion

Zinc-activated zinc oxide (ZnO:Zn) films have been prepared by screen printing of solid state sintered (100−x) wt.% ZnO−x wt.% ZnS (x: 0–15) onto ITO-coated glass substrates. Polycrystalline ZnO:Zn exhibits a hexagonal crystal structure with lattice parameters a and c decreasing slightly as the ZnS content increases. This suggests that, instead of remaining as an interstitial, the excess Zn atom occupies the oxygen vacancy of the host lattice. The CL spectra show the strongest emission line ranging from 494 to 508 nm, which is close to the green band of ZnO phosphor (510 nm). Among the various mechanisms proposed to explain the origin of the green emission band, presence of oxygen vacancies and trace ZnS residue are two possibilities for green emission in this study. However, further investigation is needed to explore both the defect formation mechanism and the green emission mechanism for ZnO:Zn phosphor. The CIE measurement and the deconvoluted CL spectra suggest that ZnO:Zn phosphor with 5 wt.% ZnS can be used to as a green primary for color picture tubes.

Acknowledgements

This work is supported by the Electronics Research and Service Organization, Industrial Technology Research Institute (ERSO, ITRI), Hsinchu, Taiwan, under contract no. E89007.

References

[1] P.H. Holloway, S. Jones, P. Pack, J. Sebastian, T. Trottier, in: Proceedings of the 10th IEEE International Symposium on Applications, Vol. 1, 1996, p. 127.
[2] A. Vecht, Display Phosphors, Vol. M-5, Society for Information Display (SID), 1999, pp. 3–48.
[3] Y.H. Tseng, B.-S. Chiou, C.C. Peng, L. Ozawa, Thin Solid Films 330 (1998) 173.
[4] C.L. Lo, J.G. Duh, B.-S. Chiou, C.C. Peng, L. Ozawa, Mater. Chem. Phys. 71 (2001) 179.
[5] B. Allieri, L.E. Depero, L. Sangaletti, L. Antonini, M. Bettinelli, Mater. Res. Soc. Symp. Proc. 508 (1998) 275.
[6] L. Ozawa, Cathodoluminescence Theory and Applications, Kodansha Ltd., Tokyo, Japan, 1990, pp. 255–261.
[7] A. Pfahnl, J. Electrochem. Soc. 109 (1962) 502.
[8] W.D. Kingery, H.K. Bowen, D.R. Uhlmann, Introduction to Ceramics, 2nd Edition, Wiley, USA, 1976, p. 58.
[9] R.C. Ropp, Luminescence and the Solid State, Elsevier, USA, 1991, p. 295.
[10] W. Lehman, J. Electrochem. Soc. 115 (1968) 538.
[11] K. Vanheusden, W.L. Warren, C.H. Seager, D.R. Tallant, J.A. Voigt, B.E. Gnade, J. Appl. Phys. 79 (1996) 7983.
[12] K. Vanheusden, W.L. Warren, C.H. Seager, D.R. Tallant, J. Caruso, M.J. Hampden-Smith, T.T. Kodas, Mater. Res. Soc. Symp. Proc. 424 (1997) 433.
[13] K. Vanheusden, C.H. Seager, W.L. Warren, D.R. Tallant, J.A. Voigt, Appl. Phys. Lett. 68 (1996) 403.